Experimental High-Frequency Parameter Identification of AC Electrical Motors

Experimental High-Frequency Parameter Identification of AC Electrical Motors

Aldo Boglietti, *Senior Member, IEEE*, Andrea Cavagnino, *Member, IEEE*, and Mario Lazzari

***Abstract*—In order to predict conducted electromagnetic interference in inverter-motor drive systems, high-frequency (HF) motor models are requested and the involved parameters have to be available. In previous studies, the authors have presented an accurate HF model for induction motors and they have defined the procedures to identify the model parameters. In this paper, these results are extended to several types and sizes of industrial ac motors such as induction, synchronous reluctance (without interior permanent magnets), and brushless motors. The model parameter-identification procedure has been improved, and it is based on a least-squares data fitting applied to the measured magnitude and phase-frequency-response curves of the phase-to-ground and the phase-to-neutral impedances. The aim of this paper is to provide quick indications to select the suitable values of the HF model parameters, with reference to the size and type of the ac motor, to evaluate the HF voltage and current components in inverted-fed ac motor systems.**

***Index Terms*—AC electrical motor, high-frequency (HF) model, parameter identification.**

I. Introduction

IN THE MODERN pulsewidth-modulation (PWM) variable-frequency ac motor drives, the switching frequencies are generally very high (up to tens of kilohertz). This means that the high-frequency (HF) components of the inverter output voltage involve electromagnetic-interference (EMI) problems, such as terminal motor overvoltage in long cable drives and HF leakage currents which flow in the stray distributed capacitances of the cable and of the motor. Due to international standards concerning the electromagnetic compatibility [2], [3], designers and users are very interested to predict these phenomena with an acceptable accuracy. In order to predict the conducted EMI, HF models of the whole main inverter cable motor system have to be considered [5], [6], [9]. In any case, the HF motor behavior plays a key role in determining the conducted EMI.

Starting with the general-purpose HF motor model reported in [1], attention is paid to the HF model of several types of ac motors. In particular, different types and sizes of induction, synchronous reluctance (synchrel), and brushless motors have been considered.

Paper IPCSD-06-090, presented at the 2005 IEEE International Electric Machines and Drives Conference, San Antonio, TX, May 15–18, and approved for publication in the IEEE Transactions on Industry Applications by the Electric Machines Committee of the IEEE Industry Applications Society. Manuscript submitted for review November 2, 2005 and released for publication September 1, 2006. This work was supported by the Ministero dell'Istruzione Università e Ricerca (MIUR) under the COFIN2003 program.

The authors are with the Dipartimento di Ingegneria Elettrica, Politecnico di Torino, 10129 Turin, Italy (e-mail: aldo.boglietti@polito.it; andrea@cavagnino@polito.it; mario.lazzari@polito.it).

Digital Object Identifier 10.1109/TIA.2006.887313

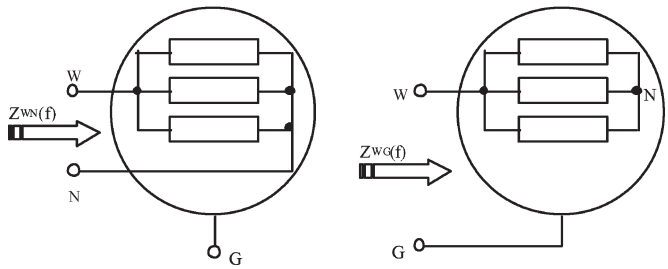

Fig. 1. Connection layout for the phase-to-neutral $[Z_{\rm WN}(f)]$ and the phase-to-ground $[Z_{\rm WG}(f)]$ impedance measurements.

The model parameters have been identified through the frequency response of the phase-to-ground $[Z_{\rm WG}(f)]$ and the phase-to-neutral $[Z_{\rm WN}(f)]$ motor impedances (Fig. 1). A least-squared data-fitting procedure has been applied to the measured magnitude and phase-impedance response curves.

As shown in the technical literature [4]–[10], frequency components higher than 1 Mhz are not able to deeply penetrate in the motor windings. For this reason, the impedance-frequency responses have been measured in the range 1 kHz–1 MHz using a standard programmable RLC meter.

The performed analysis shows that in the considered frequency range the HF-motor behavior can be simulated with lumped-parameter-equivalent circuits. As a consequence, it is possible to analyze the HF phenomena with a reasonable accuracy using standard electrical network simulation software.

The main target of this paper is to test and analyze a high number of several types of ac motors. In fact, the identified HF-motor parameters provided by this paper can be considered as a useful reference database for the drive designers interested on conducted EMI problems in inverted-fed ac-motor systems.

II. HF Lumped-Parameter Models for AC Motors

The HF lumped equivalent circuits for induction motors have been already proposed and deeply analyzed in [1]; for convenience, these equivalent single-phase circuits are shown in Fig. 2. These circuits are different for the branch constituted by the $R_{\rm se}$ and $L_{\rm se}$ parameters only. These parameters take into account the skin effect for the stator and rotor leakage inductances. The lumped parameters considered in Fig. 2 are

L_d	phase leakage inductance;
C_g	capacitance representing the winding-to-ground distributed capacitances;
R_e	resistance representing eddy currents inside the magnetic core and the motor frame;
$R_{\rm se}$, $L_{\rm se}$	$R-L$ dipole modeling the skin effect.

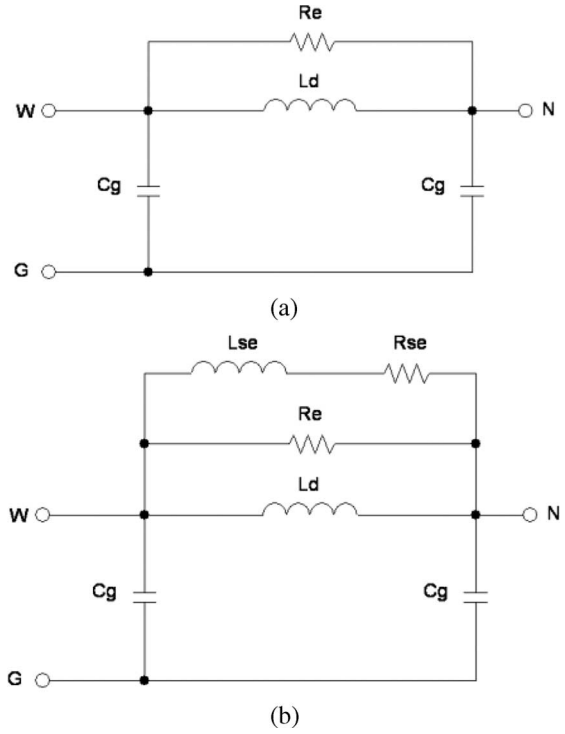

Fig. 2. Single-phase HF equivalent circuits. (a) Without the skin-effect branch. (b) Model taking into account the skin effects.

TABLE I
TYPES AND SIZES OF THE TESTED AC MOTORS

Type	Power [kW]	Motor code	Type	Power [kW]	Motor code
Induction	4	IFI-01	Induction	1.5	IEA-01
Induction	7.5	IFI-02	Induction	2.2	IEA-02
Induction	11	IFI-03	Induction	3	IEA-03
Induction	11	IFI-04	Induction	4	IEA-04
Induction	15	IFI-05	Synchrel (*)	2.2	SREA-01
Induction	18.5	IFI-06	Synchrel (*)	4	SREA-02
Induction	18.5	IFI-07	Brushless (*)	3.7	BAB-01
Induction	30	IFI-08	Brushless (*)	4.7	BAB-02
Induction	55	IFI-09	Synchrel (*)	3.8	SRAB-01
Induction	7.5	IFE-01	Synchrel (*)	3.1	SRAB-02

(*) For these motors the motor power has been calculated as the product of the continuative stall torque for the rated speed.

In [1] has been verified that the stator-winding phase resistance and the turn-to-turn distributed-capacitive coupling can be neglected in the HF motor model. It is important to underline that all the parameter values are referred to a single phase of a star-connected motor. In this paper, the models, originally developed for induction motors, have been also applied for other types of ac motors. This is possible because, in the considered frequency range, the impedance-response curves for the syncrel and brushless motors are very similar to those of induction motors (see Section III).

In Table I, the types and sizes of the analyzed ac motors are reported. A motor code will be used in this paper to identify the motor type (I: induction, SR: synchronous reluctance, B: brushless) and the motor manufacturer (FI, FE, EA, or AB). The induction and synchrel motors are all four-pole machines, whereas the considered brushless motors have six poles. In particular, both the synchrel and brushless motors have distributed windings; furthermore, in the brushless motors, the permanent magnets are mounted on the rotor surface.

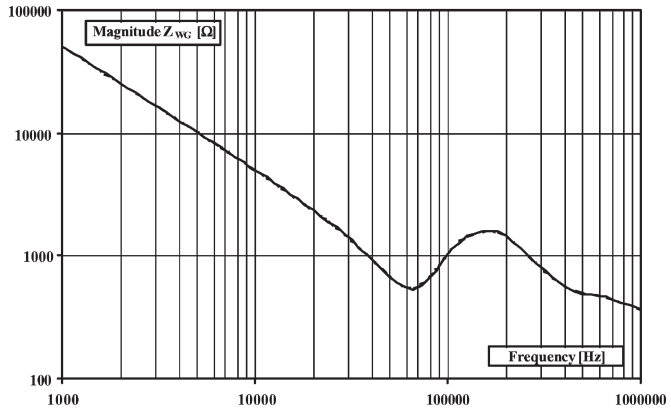

Fig. 3. Rotor position effect on the $Z_{\mathrm{WG}}(f)$ impedances of the SREA-01 motor (three overlapped curves for 0°, 22.5°, and 45° relative stator–rotor position).

It is interesting to underline that the IEA-02 and IEA-04 motors have, respectively, the same stator structure of the SREA-01 and SREA-02 ones. As a consequence, these motors allow us to analyze the squirrel-cage influences on the common-mode HF phenomena.

III. $Z_{\mathrm{WG}}(f)$ AND $Z_{\mathrm{WN}}(f)$ IMPEDANCE MEASUREMENTS

Before to start the test campaign, the influence of the rotor position on the impedance-response curves has been considered. For this reason, preliminary tests have been performed using different rotor positions, with references to the stator structure and the machine pole number. For all the considered motors, the obtained results show that and $Z_{\mathrm{WG}}(f)$ and $Z_{\mathrm{WN}}(f)$ impedances are not dependent on the rotor position. Just for example, Fig. 3 shows the $Z_{\mathrm{WG}}(f)$ frequency-response curves of the SREA-01 motor (where the rotor anisotropy is present) measured with three different rotor positions.

Using a programmable RLC meter (Hioki 3532-50) for all the considered ac motors, the $Z_{\mathrm{WG}}(f)$ and $Z_{\mathrm{WN}}(f)$ frequency-response curves (as magnitude and phase) have been measured for frequency from 1 kHz up to 1 MHz.

In Fig. 4, a comparison of the measured data for the IFI-01, IEA-04, SREA-02, and BAB-01 is shown. For the BAB-01 and BAB-02 brushless motors and for the SRAB-01 and SRAB-02 synchrel motors, the neutral point is not available. As a consequence, only the $Z_{\mathrm{WG}}(f)$ measurement is possible for these motors.

It is interesting to highligth that these four motors have quite the same power size. Then, some comparisons are possible. For example, it possible to observe that for the brushless motor the first resonance peak of $Z_{\mathrm{WG}}(f)$ is positioned at a frequency much higher than the other motors.

For some tested motors, a second resonance peak is present in the frequency-response curves (Figs. 3–5). This peak is less evident than the first one, and it is positioned at a frequency close to 1 MHz. This means that the effects of this second resonance peak can be neglected and the proposed models in Fig. 2 are suitable to describe with acceptable accuracy

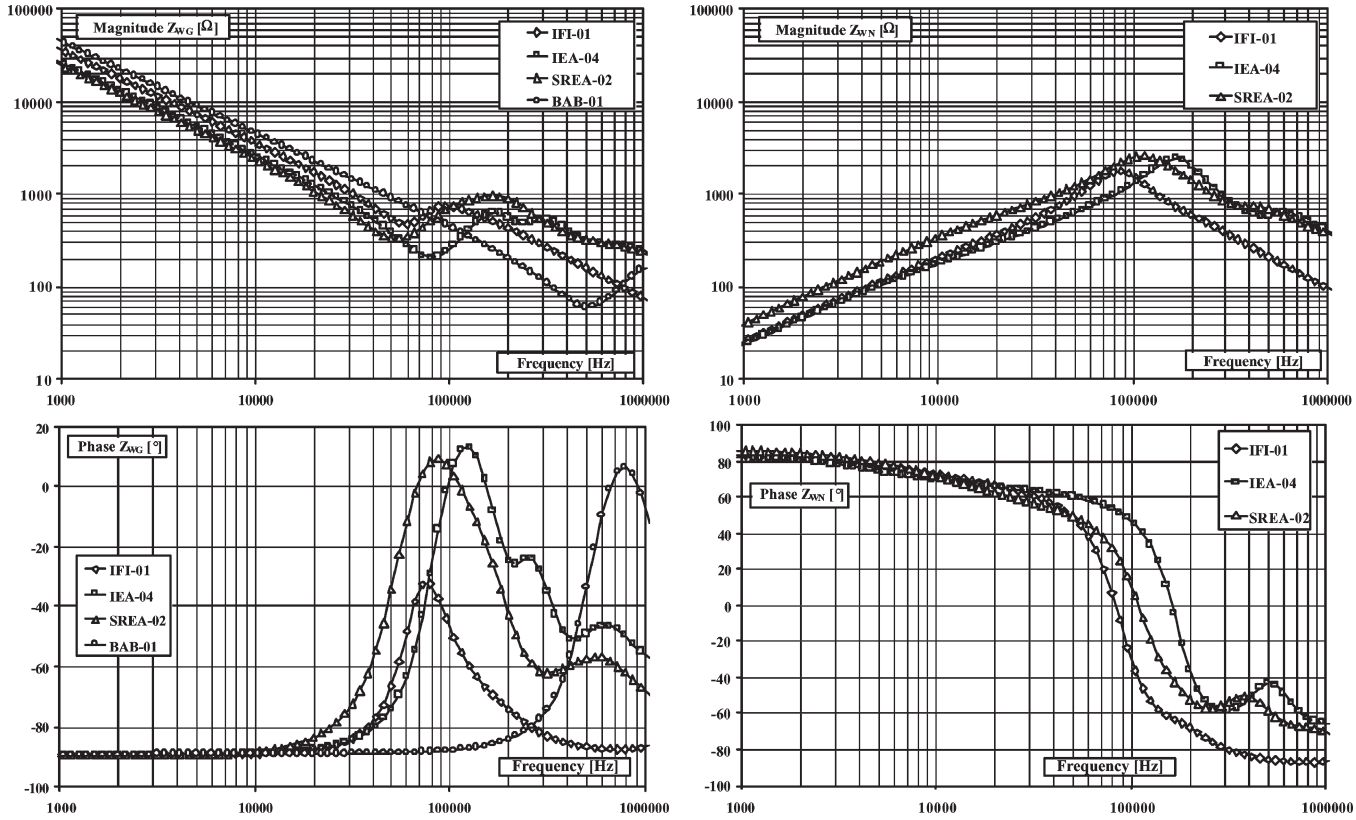

Fig. 4. Frequency-response curves for IFI-01, IEA-04, SREA-02, and BAB-01 motors: $Z_{\mathrm{WG}}(f)$ on the left side and $Z_{\mathrm{WN}}(f)$ on the right side.

the HF motor behavior in the frequency range from 1 kHz up to 1 MHz.

IV. Identification-Parameter Procedure

The circuit of Fig. 2(a) has been adopted to identify the C_g, L_d, and R_e parameters using the measured $Z_{\mathrm{WG}}(f)$ frequency-response curves. Instead, the L_{se} and R_{se} parameters have been evaluated using the measured $Z_{\mathrm{WN}}(f)$ data and the circuit reported Fig. 2(b). This choice is reasonable considering that Z_{WG} is involved in the common-mode phenomena, where the key parameter is the winding-to-ground stray capacitance, and the dipole that models the skin effect (R_{se} and L_{se} branch) is not so important.

Taking into account the motor-winding connections (Fig. 1) and the adopted equivalent circuits (Fig. 2), the Z_{WG} and Z_{WN} impedances can be calculated as shown by the expressions (1) and (2) at the bottom of the next page.

In [1] and [5], the HF model parameters have been determined through the frequency of first resonance peak in the frequency-response curve and the values of the measured impedances at low (≈1 kHz) and high (≈1 MHz) frequency.

In this paper, a different identification procedure has been implemented.

Let

$$Z(f_i) = R(f_i) + jX(f_i)$$

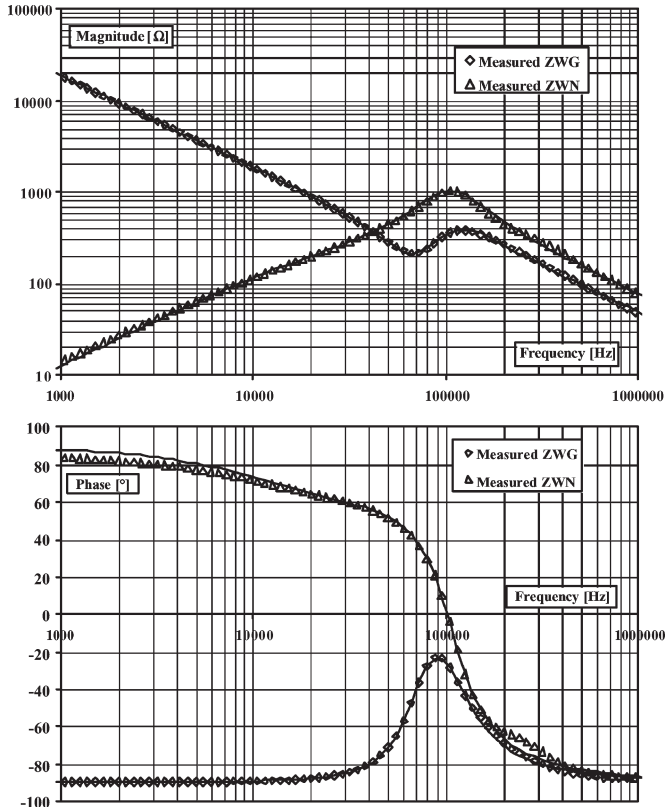

Fig. 5. Magnitude and phase of Z_{WG} and Z_{WN} for the IFI-02 motor: measured (squares and triangles) and fitted (continuous lines) frequency-response curves.

the measured data set (where "f_i" is the ith frequency value)

$$Z^*(s) = \frac{N(s)}{D(s)}$$

the unknown best model for the measured data ($N(s)$ and $D(s)$ polynomials have to be the same order of (1) and (2), respectively, for $Z_{\rm WG}$ and $Z_{\rm WN}$).

The $Z^*(s)$ transfer function is determined minimizing with the least-square method the quantity shown as follows:

$$\min \sum_{i=1}^{n} w(f_i) \cdot |Z(f_i) \cdot D(f_i) - N(f_i)|^2 . \qquad (3)$$

In (3), "n" is the sample total number of the measured data set and "$w(f_i)$" is the vector of the sample weights. Because the model has been adopted *a priori*, an accurate choice of the sample weights is very important to obtain a good fitting of the measured data.

From a practical point of view, the selection of the weight values is not a simple task. As a general comment, the authors have followed a "trial-and-error" procedure using heavier weight values for the samples near the first resonance peak of the frequency-response curves. In any case, many attempts in the weight selection are generally request to obtain good fittings.

It is important to observe that the least-squared method (3) requires calculations in complex domain. In other words, with the proposed procedure, the magnitude and phase-impedance-response curves are simultaneously involved to identify the HF model parameters.

In Fig. 5, an example of the measured (squares and triangles) and the fitted (continuous lines) frequency-response curves for the IFI-02 motor are reported. The agreement between the measured and simulated trends is well evident.

When the numerator and denominator coefficients of $Z^*(s)$ are known, it is very simple to calculate the HF-motor-model parameters through the numerator and denominator coefficients of (1) and (2). The HF model parameters estimated with the proposed procedure are reported in Table II.

About the obtained parameter values, it is important to underline that 1) the HF-parameter values are depending on the technological process used by the manufacturers. As an example, the C_g capacitance depends on the winding realization (insulation material, impregnation resin, etc.). As a consequence, the same motor manufactured by different factory can be described with a different HF-parameter set. 2) The models have been validated up to 1 MHz (maximum test frequency).

TABLE II
HF MODEL PARAMETERS FOR THE TESTED AC MOTORS

Motor code	Power [kW]	C_g [nF]	L_d [mH]	R_e [kΩ]	R_{se} [kΩ]	L_{se} [mH]
IFI-01	4	0.690	10.2	6.32	3.10	18.8
IFI-02	7.5	1.10	4.73	3.25	1.61	7.7
IFI-03	11	1.34	1.14	1.21	0.719	1.58
IFI-04	11	1.78	0.980	0.95	0.659	1.63
IFI-05	15	1.72	0.693	0.885	0.562	1.00
IFI-06	18.5	1.28	3.64	2.26	0.936	5.83
IFI-07	18.5	1.79	0.161	0.498	0.957	8.27
IFI-08	30	2.95	0.476	0.445	0.277	0.886
IFI-09	55	2.79	0.217	0.316	1.55	0.361
IFE-01	7.5	0.953	12.5	7.54	3.0	32.1
IEA-01	1.5	0.274	18.3	18.2	5.3	24.0
IEA-02	2.2	0.273	17.5	17.3	4.5	28.0
IEA-03	3	0.305	13.3	12.7	4.0	16.4
IEA-04	4	0.374	10.2	9.0	2.8	9.4
SREA-01	2.2	0.213	28.0	18.7	2.8	26.3
SREA-02	4	0.316	27.6	12.5	3.5	23.8
BAB-01	3.7	0.267	0.335	1.84	-	-
BAB-02	4.7	0.257	0.303	1.80	-	-
SRAB-01	3.8	0.207	1.67	2.63	-	-
SRAB-02	3.1	0.198	1.60	2.93	-	-

V. HF MOTOR-PARAMETER ANALYSIS

As a general comment, it is important to remember that the frequency response of the $Z_{\rm WG}$ and $Z_{\rm WN}$ impedances can be considered as standard tests for the determination of the HF-motor parameters [1], [5]–[7].

On the base of the results shown in Table II, it is possible to carry out an interesting analysis of the HF-motor parameters with reference to the motor rated power and the motor typology.

A. Induction-Motor HF Model Parameters

Due to the high number of tested induction motors, it is possible to put in evidence some interesting trends for the HF parameters with reference to the motor rated power.

The values of the capacitance C_g and inductance L_d (see Table II) as a function of the motor rated power are, respectively, shown in Figs. 6 and 7. In the same figures, the equations of the fitting curves are reported.

B. Squirrel-Cage Influence on HF Induction-Motor Parameters

Since the IEA-02 and IEA-04 induction motors have, respectively, the same stator of the SREA-01 and SREA-02 synchronous reluctance motors, it is possible to investigate the role that the squirrel cage plays in common-mode HF components.

$$Z_{\rm WG}(s) = \frac{1}{3} \frac{\frac{s^2}{C_g} + \frac{s}{C_g^2 R_e} + \frac{s}{C_g^2 L_d}}{s^3 + 2\frac{s^2}{C_g R_e} + 2\frac{s}{C_g L_d}} \qquad (1)$$

$$Z_{\rm WN}(s) = \frac{1}{3} \frac{2\frac{s^2}{C_g} + 2\frac{sR_{\rm se}}{C_g L_{\rm se}}}{s^3 + s^2\left(\frac{R_{\rm se}}{L_{\rm se}} + \frac{2}{C_g R_e}\right) + 2s\left(\frac{1}{C_g L_d} + \frac{R_{\rm se}}{C_g L_{\rm se} R_e} + \frac{1}{C_g L_{\rm se}}\right) + \frac{2R_{\rm se}}{C_g L_d L_{\rm se}}} \qquad (2)$$

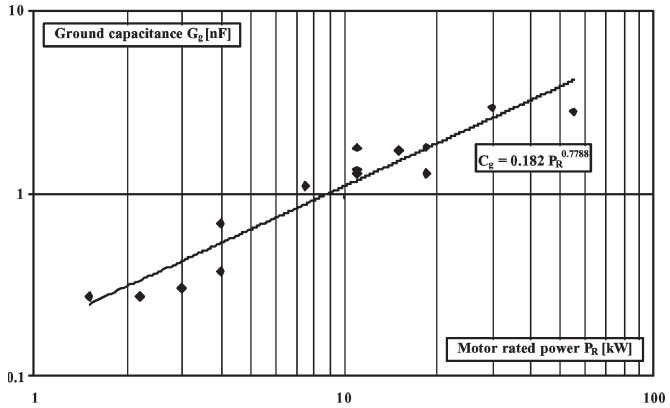

Fig. 6. Capacitance C_g as function of the motor rated power (induction motors).

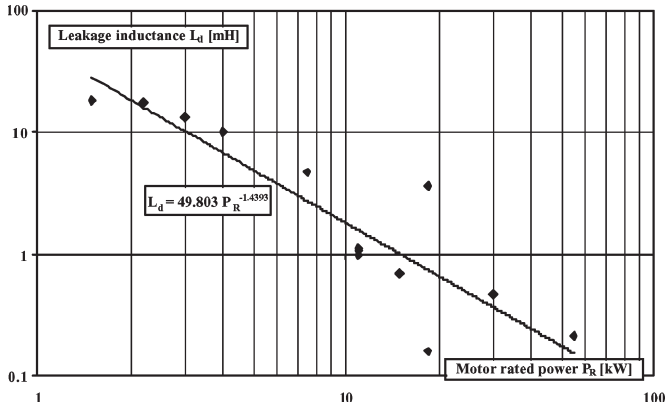

Fig. 7. Inductance L_d as function of the motor rated power (induction motors).

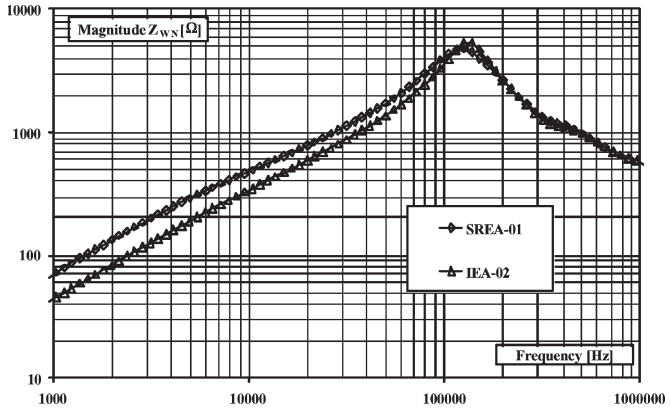

Fig. 8. Z_{WN} frequency-response curves for SREA-01 and IEA-02.

As shown in Table II, it is possible to conclude that the HF parameter mainly influenced by the squirrel-cage presence is the leakage inductance L_d. In fact, when the induction-motor stator windings are common-mode connected, the airgap magnetic fields due to the magnetomotive force space harmonics are damped by the squirrel cage. As a consequence, for the induction motors, the HF leakage inductances results lower than those of the synchrel motors. This means that the Z_{WN} frequency-response curves are quite different in the low-frequency range (Fig. 8) for the machines under study (same stator and different rotor).

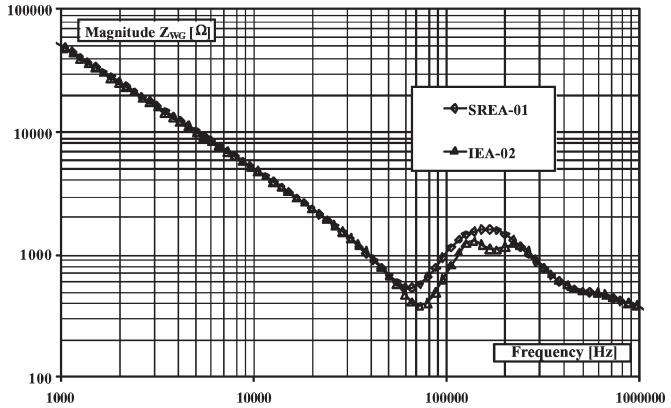

Fig. 9. Z_{WG} frequency response curves for SREA-01 and IEA-02.

TABLE III
HF MODEL PARAMETERS FOR INDUCTION MOTORS WITHOUT ROTOR

Motor code	Power [kW]	C_g [nF]	L_d [mH]	R_e [kΩ]	R_{se} [kΩ]	L_{se} [mH]
IFI-01	4	0.764	6.06	9.84	1.47	10
IFI-02	7.5	1.28	2.53	5.32	1.55	9.7
IFI-03	11	1.36	0.766	1.63	0.642	1.35

Because the other HF parameters are less dependent by the squirrel-cage presence, the $Z_{\mathrm{WG}}(f)$ curves for induction and synchrel motors with the same stator are much more similar, in particular, for lower frequency values (see Fig. 9).

C. Analysis of the L_d and C_g Parameters

For motor with the same rated power, Table II shows that L_d parameter is principally related to the rotor structure, whereas C_g parameter is practically constant.

Brushless motors have the lowest L_d values due to their large equivalent airgap (the permanent-magnet permeability is near equal to the vacuum one). In synchrel and induction machines, the airgap length is very small and the leakage inductance values are higher.

Since C_g seems not to depend on the rotor type, tests on three induction motors without the rotor have been performed. In these tests, the end caps are assembled on the motor frame. The results of these measurements are reported in Table III.

As expected by the previous considerations, L_d values with extracted rotor are lower than the ones reported in Table II.

By comparing Tables II and III, it is possible to conclude that the ground-stray capacitance C_g is practically independent by the rotor structure and it depends only by the stator one.

VI. FINAL REMARKS

The presented results confirm that the proposed lumped-equivalent circuit is suitable to describe with acceptable accuracy the HF behaviors of different types of ac motors in the frequency range from 1 kHz up to 1 MHz. It is important to underline that other more complex HF models can be defined, but in this case, the parameter identification and the physical interpretation of the parameters can be very difficult to carry out [6], [11]. The proposed model may be considered as the HF

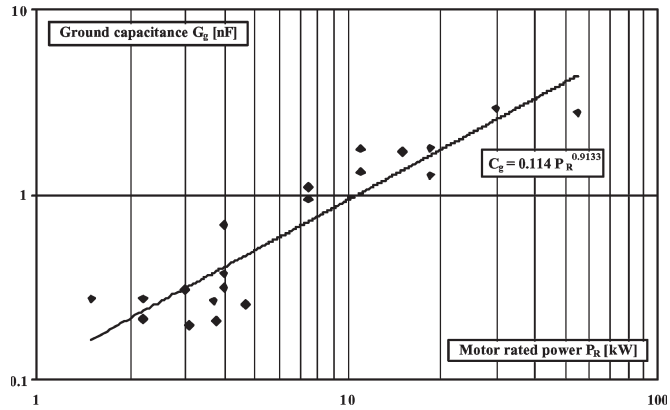

Fig. 10. Capacitance C_g versus the motor rated power (all tested motors).

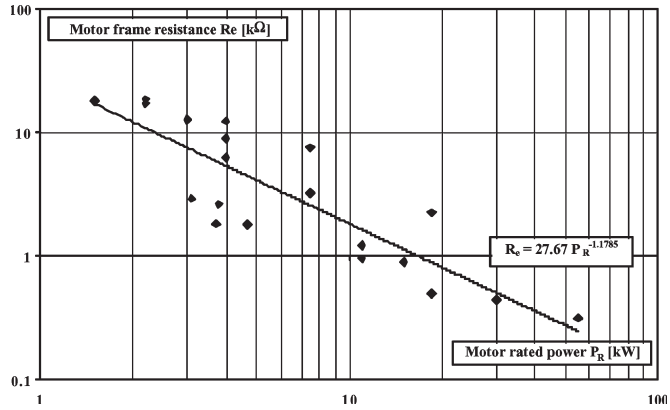

Fig. 11. Motor frame resistance R_e versus the motor rated power (all tested motors).

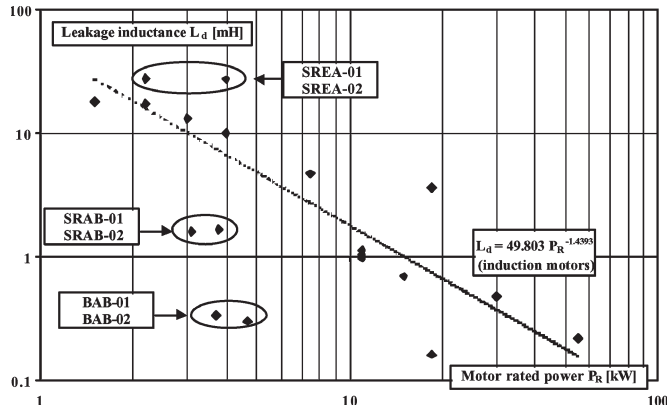

Fig. 12. Leakage inductance L_d versus the motor rated power (all tested motors).

model with the minimum number of parameters, where all the parameters can be interpreted by the physical point of view.

In the HF common-mode current evaluation, the C_g and R_e parameters play a key role, whereas the L_d, $R_{\rm se}$, and $L_{\rm se}$ parameters are less important [1]. Figs. 10 and 11 report the values of the C_g and R_e parameter of the tested motors versus the rated power. In these figures, the regression trends are reported too.

As previously highlighted, the L_d parameter depends on the rotor structure. Fig. 12 puts into evidence that the brushless

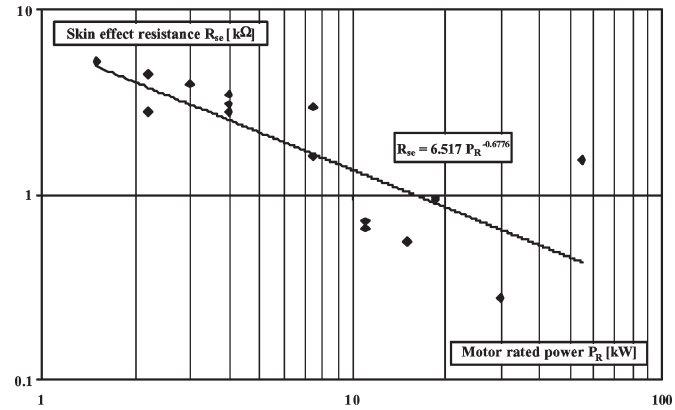

Fig. 13. Skin-effect resistance $R_{\rm se}$ versus the motor rated power (all tested motors).

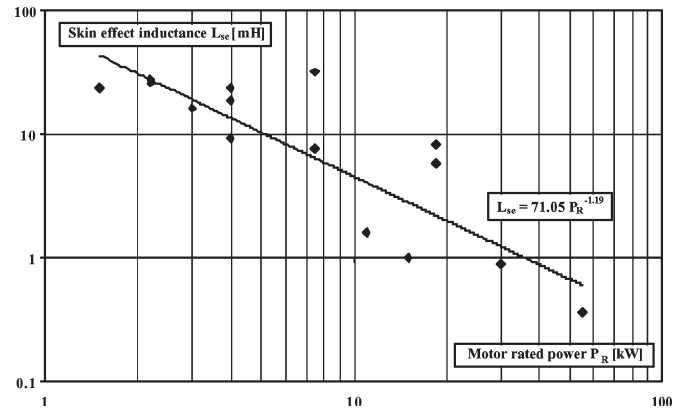

Fig. 14. Skin-effect inductance $L_{\rm se}$ versus the motor rated power (all tested motors).

motors are characterized by the smallest leakage-inductance values. The tested synchrel machines have been provided by two manufacturers, and they have L_d values quite far respect to the fitting curve reported in Fig. 12. It is important to underline that the SREA-01 and SREA-02 motors have a total enclosed fan-cooled stator frames, whereas the SRAB-01 and SRAB-02 ones have a servomotor-stator frame.

Figs. 13 and 14 allow a selection of the $R_{\rm se}$ and $L_{\rm se}$ values when the skin effect in the HF-motor model has to be taken into account.

The main goal of this paper is to systemize the HF equivalent-circuit parameter values with reference to the size and type of several ac motors. In the range of 1 kHz–1 MHz, the proposed models are able to estimate the $Z_{\rm WG}(f)$ and $Z_{\rm WN}(f)$ motor impedances with acceptable accuracy. It is important to underline that the accuracy of the proposed HF models in the time domain have been already analyzed and discussed in [1], where several considerations about the HF-motor model supplied by triangular voltage and PWM inverter voltage can be found.

The proposed model represents a simple solution to the analysis of HF ac motor drive problems linked to conducted EMI, and its validity has been recognized by other researchers [5], [12]. About the model-parameter identification, the adopted "trial and error" procedure could seem a trivial approach, but

it is very fast and practical (in particular from an engineering point of view), when the results of the impedance–frequency responses are available.

VII. Conclusion

In this paper, the HF-parameter identification of several types of ac electrical motors, based on a full experimental approach, is presented. In particular, induction, synchronous reluctance, and brushless motors have been considered. Lumped-parameter single-phase equivalent circuits are used to analyze the HF behavior of ac motors. This paper shows that the model is not dependent on the ac motor types.

The HF-motor parameters are evaluated through measurements of magnitude and phase of phase-to-ground and phase-to-neutral impedances performed in the frequency range from 1 kHz up to 1 MHz. The adopted parameter-identification procedure, based on a least-squares data fitting performed in complex domain, is reported in detail together with the estimated parameters.

With reference to the size and type of ac motors, a critical analysis of the numerical values of the obtained parameters has been carried out.

The motor HF model plays an important role in the HF analysis when the machine is supplied by inverter source. For these reasons, this paper can be considered as a useful starting point for the designers interested on conducted EMI problems in inverted-fed ac motor drives.

References

[1] A. Boglietti and E. Carpaneto, "An accurate induction motor high-frequency model for electromagnetic compatibility analysis," *Electr. Power Compon. Syst.*, vol. 29, no. 3, pp. 191–209, Mar. 2001.

[2] *Adjustable Speed Electrical Power Drive Systems—Part 3: EMC Product Standard Including Specific Test Methods*, IEC 61800-3, 1996-09.

[3] *Industrial, Scientific and Medical (ISM) Radio-Frequency Equipment—Electromagnetic Disturbance Characteristics—Limits and Methods of Measurement*, IEC CISPR 11 Ed.4.1, 2004-06.

[4] G. Grandi, D. Casadei, and A. Massarini, "High frequency lumped parameter model for AC motor windings," in *Proc. EPE Conf.*, Trondheim, Norway, 1997, vol. 2, pp. 578–583.

[5] A. F. Moreira, T. A. Lipo, G. Venkataramanan, and S. Bernet, "High-frequency modeling for cable and induction motor overvoltage studies in long cable drives," *IEEE Trans. Ind. Appl.*, vol. 38, no. 5, pp. 1297–1306, Sep./Oct. 2002.

[6] L. Ran, S. Gokani, J. Clare, K. J. Bradley, and C. Christopoulos, "Conducted electromagnetic emission in induction motor drive system—Part I: Time domain analysis and identification of dominant modes," *IEEE Trans. Power Electron.*, vol. 13, no. 4, pp. 757–767, Jul. 1998.

[7] ——, "Conducted electromagnetic emission in induction motor drive system—Part II: Frequency domain models," *IEEE Trans. Power Electron.*, vol. 13, no. 4, pp. 768–776, Jul. 1998.

[8] E. Zhong and T. A. Lipo, "Improvements in EMC performance of inverter-fed motor drives," *IEEE Trans. Ind. Appl.*, vol. 31, no. 6, pp. 1247–1256, Nov./Dec. 1995.

[9] G. Skibinski, R. Kerkman, D. Leggate, J. Pankau, and D. Schlegel, "Reflected wave modeling techniques for PWM AC motor Drives," in *Proc. IEEE APEC*, Feb. 1998, vol. 2, pp. 1021–1029.

[10] A. Consoli, G. Oriti, A. Testa, and A. L. Julian, "Induction motor modeling for common mode and differential mode emission evaluation," in *Conf. Rec. IEEE IAS Annu. Meeting*, Oct. 1996, vol. 1, pp. 595–599.

[11] M. Cacciato, A. Consoli, L. Finocchiaro, and A. Testa, "High frequency modeling of bearing currents and shaft voltage on electrical motors," in *Proc. ICEMS*, Sep. 27–29, 2005, vol. 3, pp. 2065–2070.

[12] I. Boldea and S. A. Nasar, *The Induction Machine Handbook*. Boca Raton, FL: CRC Press, 2002, pp. 729–751.

Aldo Boglietti (M'04–SM'06) was born in Rome, Italy, in 1957. He received the Laurea degree of electrical engineering from the Politecnico di Torino, Turin, Italy, in 1981.

He started his research work with the Department of Electrical Engineering, Politecnico di Torino, as a Researcher in electrical machines in 1984. He became an Associate Professor of electrical machines in 1992, and has been a Full Professor since November 2000. He is also currently the Head of the Electrical Engineering Department of the Politecnico di Torino, until 2007. He is the author of about 100 papers and his research interests include energetic problems in electrical machines and drives, high-efficiency industrial motors, magnetic materials and their applications in electrical machines, electrical machines and drives models, and thermal problems in electrical machines.

Andrea Cavagnino (M'04) was born in Asti, Italy, in 1970. He received the M.Sc. and Ph.D. degrees in electrical engineering from the Politecnico di Torino, Turin, Italy, in 1995 and 1999, respectively.

Since 1997, he has been with in the Electrical Machines Laboratory of the Department of Electric Engineering, Politecnico di Torino, where he is currently an Assistant Professor. His fields of interest include electromagnetic design, thermal design, and energetic behaviors of electric machines. He has authored several papers published in technical journals and conference proceedings.

Dr. Cavagnino is a Registered Professional Engineer in Italy.

Mario Lazzari was born in Lucca, Italy, in 1945. He received the Laurea degree in electrical engineering from the Politecnico di Torino, Turin, Italy, in 1969.

In 1970, he joined the Department of Electrical Engineering, Politecnico di Torino, where he is currently a Full Professor of Electrical Machines and Drivers. From 1991 to 1993, he was the Chairman of the Laurea Course of Electrical Engineering. His research interests include dynamics of electrical machines and electromechanical design, particularly in regard to energetic problems. He is the author of several technical papers on these topics.